Nanoscale Electroless Metal Deposition in Aligned Carbon Nanotubes

Jing Li, Martin Moskovits, and Tom L. Haslett*

Department of Chemistry, University of Toronto, 80 St. George St., Toronto, Canada M5S 3H6

Received March 3, 1998. Revised Manuscript Received May 12, 1998

Arrays of aligned, multiwalled carbon nanotubes were produced by catalytically pyrolyzing acetylene within the pores of an anodic aluminum oxide template. Small cobalt catalyst particles were predeposited electrochemically at the bottom of the pores. The tube walls consisted of approximately 10 carbon layers with an interlayer spacing of approximately 3.45 Å, somewhat larger than the 3.35 Å interplanar spacing of graphite. The nanotubes were found to be open at one end, making it possible fill the tubes with metals or other materials. Nickel and cobalt metals were deposited in the interior of the tubes using nanoscale electroless deposition. The deposited metals included small quantities of phosphorus or boron, according to the reducing agent used in the electroless deposition process (hypophosphite or dimethylamine−borane). The deposits in general consisted of discontinuous, polycrystalline metal filling most of the length of the nanotube, but in the case of Co reduced with hypophosphite, continuous polycrystalline deposits of up to 3 μm were observed. The Ni crystallites inside the tubes had fcc structures with cell constants of 3.56 Å, slightly larger than the 3.52 Å lattice constant of bulk nickel possibly due to the inclusion of P.

Introduction

The growth of carbon nanotubes, until recently referred to as filamentous carbon, has been extensively studied in the past.[1] Because of its key role in catalyst poisoning, the principle aim of the research was to avoid its formation. More recently, nanotubes have been the subject of a great deal of exciting research due to their potentially unique electronic and mechanical properties.[2−7] The results of numerous theoretical and experimental studies suggest that by changing the structural characteristics of the nanotubes, materials possessing a wide range of physical properties may be synthesized.[3−7] One drawback to their study and eventual commercial application has been the rather haphazard manner in which nanotubes are normally fabricated. Recently, advances in the synthesis of nanotubes were reported by Terranes et al., who generated aligned nanotubes by pyrolyzing a hydrocarbon on a patterned cobalt catalyst deposited on a silica substrate.[8] Likewise, Li et al. used iron nanoparticles deposited in mesoporous silica to generate arrays of nanotubes.[9] Porous anodic aluminum oxide (AAO) templates, commonly used for preparing arrays of nanowires, have also been applied to the fabrication of nanotubes. Martin et al.,[10] for example, produced carbon nanotubes in AAO templates by depositing polyacrylonitrile in the pores and subsequently thermally decomposing the polymer, while Kyotani et al.[11] achieved similar results by pyrolyzing propylene.

The possibility of producing metal or semiconductor-filled carbon nanotubes is of even greater potential technological interest than the tubes themselves. Systems with potentially novel magnetic or electronic properties may result thereby.[12] The hollow interiors of the nanotubes might then be thought of as nanometer-sized test tubes, in which a variety of submicroscopic processes might be carried out.[13,14] Small particles of some 15 metals (including Fe, Co, Ni, Ti, Cu, and a few rare earth metals and metal carbides) have been successfully encapsulated in carbon nanotubes by including the metals in the carbon arc commonly used

(1) See, for example: Baker, R. T. K.; Chludzinski, J. J., Jr.; Lund, C. R. F. *Carbon* **1987**, *25*, 295. Baker, R. T. K.; Chludzinski, J. J., Jr.; Dudash, N. S.; Simoens, *A. J. Carbon* **1983**, *21*, 463. Also, see the thorough review of Baker, R. T. K.; Harris, P. S. In *Chemistry and Physics of Carbon*, Vol. 14; Walker, P. L., Thrower. P. A., Eds.; Dekker: New York, 1978, and references therein.

(2) Iijima, *S. Nature* **1991**, *354*, 56.

(3) Treacy, M. M. J.; Ebbesen, T. W.; Gibson, J. M. *Nature* **1996**, *381*, 678.

(4) Ebbesen, T. W.; Lezec, H. J.; Hiura, H.; Bennett, J. W.; Ghaemi, H. F.; Thio, T. *Nature* **1996**, *382*, 54.

(5) Dresselhaus, M. S.; Dressehlaus, G.; Eklund, P. C. *Science of Fullerenes and Carbon Nanotubes*; Academic Press: New York, 1985; pp 757−869.

(6) Saito, R.; Dresselhaus, G.; Dresselhaus, M. S. *J. Appl. Phys.* **1993**, *73*, 494.

(7) Dai, H.; Hafner, J. H.; Rinzler, A. G.; Colbert, D. T.; Smalley, R. *Nature* **1996**, *384*, 147.

(8) Terrones, M.; Grobert, N.; Olivares, J.; Zhang, J. P.; Terrones, H.; Kordatos, K.; Hsu, W. K.; Hare, J. P.; Townsend, P. D.; Prassides, K.; Cheetham, A. K.; Kroto, H. W.; Walton, D. R. M. *Nature* **1997**, *388*, 52.

(9) Li, W. Z.; Xie, S. S.; Qian, L. X.; Chang, B. H.; Zou, B. S.; Zhuo, W. Y.; Zhao, R. A.; Wang, G. *Science* **1996**, *274*, 1701.

(10) Parthasarathy, R. V.; Phani, K. L. N.; Martin, C. R. *Adv. Mater.* **1995**, *7*, 896.

(11) Kyotani, T.; Tsai, L.; Tomita, A. *Chem. Mater.* **1996**, *8*, 2190.

(12) Murakami, Y.; Shibata, T.; Okuyama, K.; Arai, T.; Suematsu, H.; Yoshida, Y. *J. Phys. Chem. Solids* **1993**, *54*, 1861.

(13) Ugarte, D.; Chatelain, A.; De Heer, W. A. *Science* **1996**, *274*, 1897.

(14) Tsang, S. C.; Chen, Y. K.; Harris, P. J. F.; Green, L. H. *Nature* **1994**, *372*, 159.

S0897-4756(98)00122-7 CCC: $15.00
Published on Web 07/01/1998

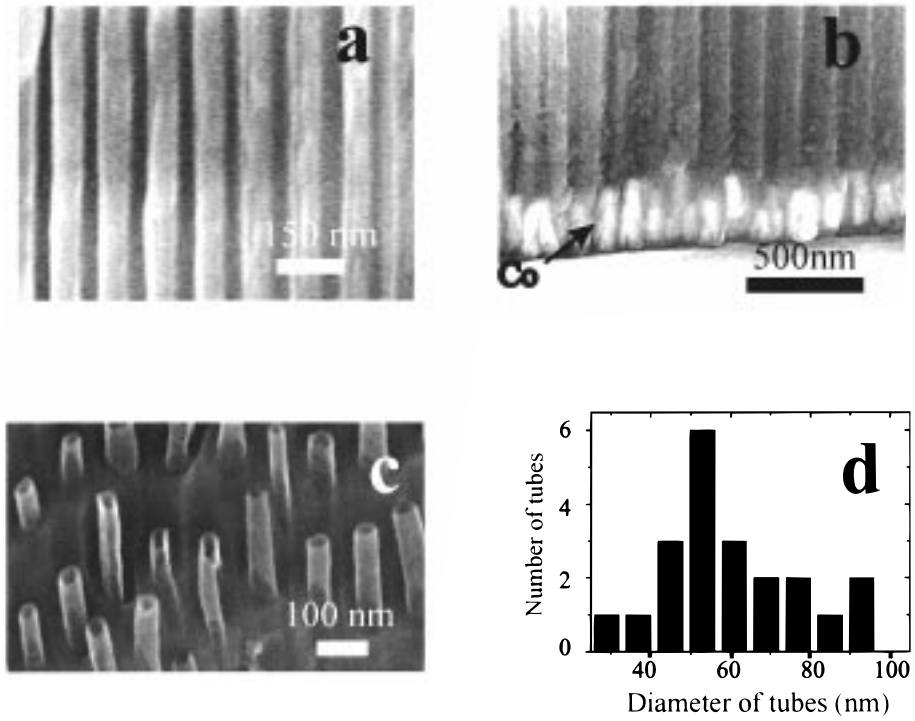

Figure 1. SEM images of (a) the empty template cross section (50 V anodization, 30 min. widening), (b) Co catalyst particles at the bottom of the pores, and (c) carbon nanotubes partially exposed by etching the surface of the alumina template with NaOH. (d) Diameter distribution of carbon nanotubes fabricated in the templates shown in (a).

to synthesize the nanotubes.[15−17] Small quantities of low-melting metals, such as lead, zinc, selenium, and molten $AgNO_3$, have also been incorporated in nanotubes through capillary action after the closed ends of the nanotubes were partially opened chemically.[13,14,18,19] However, to study this new class of materials reliably and to be able to apply them, it is essential that aligned carbon nanotubes be reproducibly synthesized in quantity, with controllable dimensions, and methods developed to fill the tubes with as wide a range of materials as possible.

To address this goal, we have developed a powerful new method for producing and filling arrays of carbon nanotubes based on the following steps. (i) Porous anodic aluminum oxide (AAO) templates are electrochemically produced by anodizing superpurity aluminum foils in a suitable acid electrolyte. The resulting oxides possess uniform, parallel pores of controllable diameter and length, with a narrow distribution of diameters.[20] (ii) A nanoparticle of cobalt is electrodeposited at the bottom of each of the pores of the template to serve as a catalyst in the subsequent pyrolysis step. (iii) Uniformly aligned carbon nanotubes are generated inside each of the pores through the catalytic pyrolysis of a suitable hydrocarbon, such as acetylene. The tubes so formed normally have an outer diameter equal to the inner diameter of the pore in which they are fabricated. (iv) The desired interior metal, such as nickel or cobalt, is deposited within the nanotubes by electroless deposition. At present, the deposited metals include P and B impurities occluded during the electroless deposition step. As plated, the Ni−P and Ni−B deposits are lamellar crystallites which are, likely, solid solutions of P or B dissolved in finely crystalline Ni. It is known that heat treatment of similar deposits at 400 °C produces an intermetallic Ni_3P precipitate with concomitant metallic grain growth.[21] The P content of our deposits was 6 at. % with a grain size of approximately 5 nm. Although we have not determined if the P or B is included homogeneously or as domains, we refer to these deposits as alloys in keeping with common practice. Matsuoka has reported crystallite sizes for electroless deposits with 3−7% P lying in the range of 1.4 to 11.9 nm, in good agreement with our observations.[22]

Experimental Section

Anodic oxidation of aluminum (99.99%) was carried out in 0.3 M oxalic acid at various anodizing voltages ranging from 25 to 65 V at 18 °C. The thickness of the anodic film was adjusted to be from 5 to 10 μm by setting the anodization time appropriately and checking it using electron microscopy. The AAO templates were then immersed in a 0.1 M phosphoric acid etching solution at 30 °C for 30 to 60 min to widen the pores and thin the oxide barrier layer at the pore bottom. Pore diameters were controlled to lie in the range 20 to 100 nm (±7 nm) by varying the anodizing voltage and etching times. A typical template oxidized at 50 V and widened for 30 min has an average pore diameter of 50 nm and very straight, uniform channels (Figure 1a).

(15) Iijima, S.; Ichihashi, T. *Nature* **1993**, *363*, 603.
(16) Saito, Y.; Yoshikawa, T.; Okuta, M.; Fujimoto, N.; Sumiyama, K.; Suzuki, K.; Nishina, Y. *J. Phys. Chem. Solids* **1993**, *54*, 1849.
(17) Guerret-Piecourt, C.; Le Bouar, Y.; Loiseau, A.; Pascard, H. *Nature* **1994**, *372*, 761.
(18) Ajayan, P. M.; Ebbesen, T. W.; Ichihashi, T.; Iijima, S.; Tanigaki, K.; Hiura, H. *Nature* **1993**, *362*, 522.
(19) Dujardin, E.; Ebbesen, T. W.; Hiura, H.; Tanigaki, K. *Science* **1994**, *265*, 1850.
(20) Routkevitch, D.; Bigioni, T.; Moskovits, M.; Xu, J. M. *J. Phys. Chem.* **1996**, *100*, 14037.
(21) Riedel, W. *Electroless Nickel Plating*; ASM International: Metals Park, Ohio, 1991.
(22) Matsuoka, M.; Imanishi, S.; Hayashi, T. *Plating Surf. Finishing* **1989**, *76*, 54.

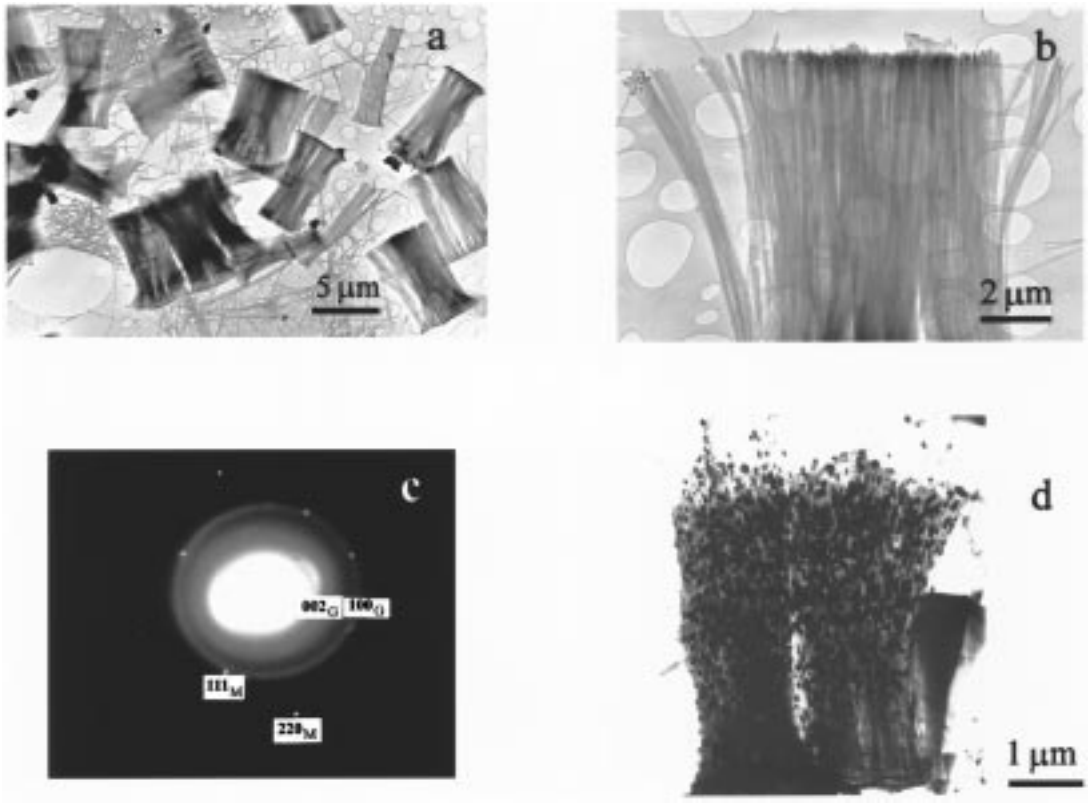

Figure 2. (a) TEM image of bundles of carbon nanotubes, 8 μm in length, extracted from their AAO template showing their lengths to be uniform and equal to the film thickness of AAO template, and (b) a close-up TEM image of one of the bundles. (c) Electron diffraction pattern of carbon nanotubes with Ni−P deposits. Miller indices, indicated with subscripts G and M, refer to graphitic carbon and the P-doped Nickel deposit, respectively. (d) TEM image of a bundle of carbon nanotubes filled with P-doped Ni metal deposited by electroless plating.

Cobalt or iron particles 100−200 nm in length (Figure 1b) were electrochemically deposited by AC electrolysis at the bottom of the pores using 14 V_{RMS} at 100 Hz for 30 s in an electrolyte consisting of 240 g/L of $CoSO_4 \cdot 7H_2O$ (or 120 g/L of $FeSO_4 \cdot 7H_2O$), 40 g/L of HBO_3, and 1 g/L of ascorbic acid. The cobalt- or iron-containing AAO templates were placed in a tube furnace and reduced at 600 °C for 4−5 h in a flow of CO (100 mL/min). Then a mixture of 10% acetylene in nitrogen was introduced into the reactor at a flow rate of 100 mL/min. The acetylene was pyrolyzed for 20 min at 700 °C to form carbon nanotubes in the template pores. Subsequently, the nanotubes were annealed at 700 °C in flowing nitrogen for 15 h in order to graphitize them further. Diagnostics on the template and the carbon nanotubes were carried out using scanning electron microscopy (SEM, Hitachi S-4500) and transmission electron microscopy (TEM, H7000 or JEOL 2021F). To prepare specimens for TEM imaging, the nanotube-containing templates were dipped in a 0.1 M NaOH solution at 60−80 °C for 3 h in order to dissolve the alumina template, thereby releasing the carbon nanotubes as an insoluble fraction. After several washings in distilled water and ethanol, a drop of an ethanol suspension of the nanotubes was placed on a TEM grid.

Results and Discussion

An SEM image of carbon nanotubes partially exposed by briefly etching the alumina template in aqueous NaOH is shown in Figure 1c. The nanotubes are perpendicular to the template, open at the top, and appear to fit the pores snugly, suggesting that their outer diameters correspond to the pore inner diameters. The pore diameters were found to increase slightly after annealing, presumably due to morphological changes in the template resulting from water loss and other chemical changes in the alumina. Consequently, the average measured nanotube diameter, at 60 nm (Figure 1d), is somewhat larger than the 50 nm average pore diameter measured at room temperature before annealing the templates.

After completely dissolving the alumina, bundles of nanotubes such as those shown in Figures 2a,b could be separated from the template. The length of the nanotubes (8 μm) corresponds exactly to the thickness of the template in which they were produced. The uniformity and parallelity of the tubes may also be gauged from the image shown in Figure 2b. An electron diffraction pattern (Figure 2c) recorded for the bundle of nanotubes shown in Figure 2d suggests an ordered graphitic structure. The interlayer separation (d_{002}) is approximately 3.45 Å, which is slightly larger than the interplanar distance in graphite (d_{002} = 3.35 Å). The tube wall thickness is measured by TEM to be approximately 3−4 nm, suggesting that the multiwalled tube consists of approximately 10 graphitic layers.

TEM images also show that the catalyst particles remain at the bottom of the pores during the reaction. We have not observed any tubes having the catalyst particle trapped within the tube. It is clear that the mechanism of tube growth is complex and some of its aspects have yet to be determined. The cobalt catalyst might promote the decomposition of the hydrocarbon throughout the entire growth process of the nanotube, in which case the tube would grow from the bottom upward; or it might merely initiate the growth of the tube through the initial catalytic decomposition of the hydrocarbon reagent, with subsequent tube growth

proceeding at the reactive "upper" periphery of the nanotube. In the former case, the role of reagent transport to the bottom of the pore might be an important rate-limiting step for narrow and/or long pores. Another potentially rate-limiting step in this model could be the transport of carbon, possibly as a carbide, through or along the surface of the metal particle to the pore wall, where tube growth occurs. Baker and co-workers have shown this process to be the rate-limiting step for carbon filaments growing from catalyst particles on a surface.[1] This appeared to be the case regardless of whether the particle was fixed to the surface or propogated with the growing end of the tube.

Since the alumina is itself a catalyst in the hydrocarbon decomposition process, albeit a far less effective catalyst than cobalt, its role further complicates the mechanism for templates with long or narrow pores. Indeed, there is evidence that different nanotube structures are produced (for example, helical nanotubes) when the pores are very short.

A novel and important characteristic of the nanotubes is the open end, corresponding to the open end of the pore (Figure 1c), which makes it possible to fill them with other materials or carry out nanoscale chemical reactions in their interior. An effective strategy for introducing metals into the interior of the nanotubes is electroless plating, a process whereby a metal coating can be continuously chemically deposited on a surface.[21]

Using electroless plating, nickel was deposited into the interior of the carbon nanotubes while they were still encapsulated in an AAO template with 60 nm average diameter. The nanotube-bearing AAO films were washed sequentially in acetone and distilled water and then immersed in an acid bath containing nickel ions and hypophosphite reducing agent for 20−30 min at 25−40 °C until a metallic color appeared.[23] Since deposition takes place where the reduction of metal ions is catalyzed by the surface, the successful deposition of nickel in the interior of the nanotubes suggests that the inner surface of the nanotube is sufficiently active to initiate the metal deposition process. The deposition location was also found to be temperature dependent. In the range 30−40 °C, deposition occurred predominantly in the interior of the nanotubes, while at higher temperatures (70−90 °C) deposition occurred almost exclusively on the surface of the template. The addition of 0.5 g/L of quinhydrone as a pH buffer was found to improve the deposition, possibly by also functioning as a surfactant, thus improving the wetting and hence the penetration of the solution into the nanotubes.

The electroless nickel deposits are not pure nickel but contain significant amounts of phosphorus, the percentage varying with the bath composition and operating conditions. Energy dispersive X-ray (EDX) analysis of the Ni−P deposits suggests an average Ni/P atomic ratio of 94:6. High-resolution TEM images (Figure 3b) show the as-plated Ni−P deposits to be polycrystalline, with crystallite sizes ranging from 3 to 5 nm. An electron diffraction pattern (Figure 2c) recorded from a bundle of Ni-containing nanotubes (Figure 2d) exhibits clear

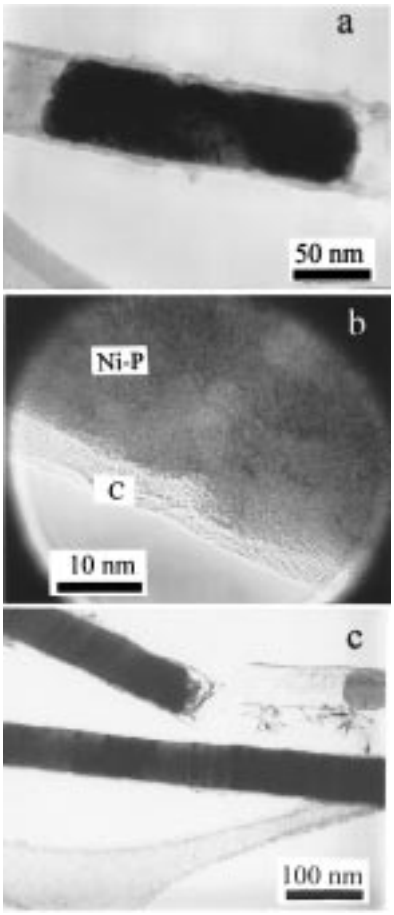

Figure 3. (a) TEM image of a Ni−P particle deposited in the interior of a carbon nanotube. (b) High-resolution TEM image of (a), showing the tube wall structure and interface. (c) TEM image of needlelike crystals of Co−P forming a continuous nanowire in the interior of a carbon nanotube. elsewhere.

diffraction spots corresponding to Ni(111) and Ni(220) reflections, from which a lattice constant of 3.56 Å was determined for the Ni−P alloy crystallites in the interior of the nanotubes. This value is marginally larger than the 3.52 Å lattice constant of bright (fcc) deposited nickel.[21] The slightly expanded lattice of the electroless deposited nickel may be due to the incorporation of phosphorus atoms into the nickel crystallites. When dimethylamine−borane was used as the reducing agent instead of hypophosphite, very similar electroless deposits of nickel alloyed with small quantities of boron were obtained in the interior of the nanotubes.

In contrast to nickel deposition, cobalt required higher temperatures for optimum deposition. Temperatures of 70 °C were best with the hypophosphite reducing agent, while 40−50 °C in an acid bath at pH 5.5 produced an optimal deposition of Co using dimethylamine−borane.[21,23] Nickel, using either reducing agent, and cobalt, using dimethylamine−borane, deposited in the interior of the nanotubes as discrete particles rather than as continuous nanowires. This is probably due to the occlusion of other reaction products in the electroless reduction process preventing the metal from forming continuous nanowires. Furthermore, growth at particularly active sites along the tube wall may block the tube at some point in the deposition, preventing electrolyte reagent from penetrating.

(23) For electroless nickel plating: 30 g/L of nickel chloride, 10 g/L of sodium hypophosphite, 50 g/L of sodium acetate and ammonia to pH 5. For electroless cobalt plating: 30 g/L of cobalt chloride, 4 g/L of dimethyamine−borane, 25 g/L of sodium acetate, pH 5.5.

Interestingly, when Co was deposited using hypophosphite as the reducing agent, the deposit appeared to consist of small needlelike crystals perpendicular to the wall of the nanotube (Figure 3c). The deposit was still discontinuous over the length of the tube, but continuous particles of up to 3 μm were commonly observed, suggesting that conditions may be found in which the entire tube can be continuously filled. The microstructure of both the cobalt−boron and cobalt−phosphorus deposits have not yet been determined since the electron diffraction patterns suggest the presence of more than one phase.

CM980122E